ELSEVIER

Inorganica Chimica Acta 339 (2002) 14–26

Inorganica Chimica Acta

www.elsevier.com/locate/ica

Interaction of (amine)M(II) complexes (amine = dien, en; M = Pd, Pt) with purine nucleoside 2′-, 3′- and 5′-monophosphates—the role of the phosphate site for specific metal fragment–nucleotide recognition by macrochelation

W. Wirth, J. Blotevogel-Baltronat, U. Kleinkes, W.S. Sheldrick *

Lehrstuhl für Analytische Chemie, Ruhr-Universität Bochum, D-44780 Bochum, Germany

Received 16 July 2001; accepted 12 October 2001

Dedicated to Professor Helmut Sigel on the occasion of his 65th birthday

Abstract

The pH-dependent interaction of $[Pd(dien)(H_2O)]^{2+}$ with adenosine and guanosine 2′- and 3′-monophosphates at molar ratios $R = 1$ and 3 has been studied by potentiometric and NMR techniques. The absence of additional intramolecular stabilisation of the N7 coordination mode by (amine)N–H···O(phosphate) hydrogen bonding, as for 5′-AMP^{2-} or 5′-GMP^{3-}, leads to reversal of the intrinsic binding ratio log [β(BM_1)/β(M_7B)] in favour of N1 coordination for mononuclear (dien)Pd(II) complexes of the purine 2′- and 3′-nucleotides. Outer-sphere κ^2N7,O(phosphate) macrochelation is also responsible for the formation of a specific μ-*N1*,*N7* bridged cyclic tetramer $[\{(en)Pd(5'\text{-}GMP)\}_4]^{4-}$ in the pH range 5.5–9.5. Both inner- and outer-sphere κ^2N3,O(phosphate) macrochelation lead at $R = 3$ to a dramatic enhancement of (en)Pd(II) binding to N3 of 2′-GMP^{3-} in comparison to 3′- or 5′-GMP^{3-}. Reaction of $[\{Pt(dien)\}_2(2'\text{-}GMP\text{-}\mu\text{-}N1,N7)]^{+}$ with $[Pt(en)(H_2O)_2]^{2+}$ affords both types of macrochelate at approximately 1:1 ratio, namely $[\{Pt(dien)\}_2(2'\text{-}GMP\text{-}\mu_3\text{-}N1,N3,N7,O(P))\{Pt(en)\}^{3+}$ and $[\{Pt(dien)\}_2(2'\text{-}GMP\text{-}\mu_3\text{-}N1,N3,N7)\ \{Pt(en)H_2O)\}]^{3+}$ with respectively direct (en)Pt–O(phosphate) and outer-sphere (amine)N–H···O(phosphate) hydrogen bonding. Following HPLC separation, these trinuclear products could be characterised by NMR and FAB-MS.
© 2002 Elsevier Science B.V. All rights reserved.

Keywords: Purine nucleotides; Palladium complexes; Platinum complexes; Macrochelation

1. Introduction

It is well documented [1–7] that intramolecular N–H···O(P) hydrogen bonding plays an important role in stabilising N7-coordinated (amine)M(II) complexes (M = Pd, Pt) of 5′-GMP^{3-} and 5′-IMP^{3-} in solution. X-ray crystal structure determinations have confirmed this outer-sphere macrochelation mode in $[M(en)(5'\text{-}GMPH\text{-}\kappa N7)_2]\cdot 9H_2O$ [5] and $[Pd(en)(5'\text{-}IMPH\text{-}\kappa N7)_2]\cdot 11H_2O$ [6] and Uchida et al. have proposed that such interactions are responsible for the formation of a specific tetramer $[\{Pd(en)(5'\text{-}GMP\text{-}\mu\text{-}N1, N7)\}_4]^{4-}$ at neutral pH [3]. The stabilisation of intermediates through intramolecular N–H···O(phosphate) hydrogen bonding is also considered to be responsible [8] for the significantly faster reaction of *cis*-$[Pt(NH_3)_2(H_2O)_2]^{2+}$ with 5′-GMP^{3-} or 5′-$dGMP^{3-}$ in comparison to 3′-GMP^{3-} or guanosine [9,10] (Scheme 1).

Although the binding equilibria of the model complexes $[Pd(dien)(H_2O)]^{2+}$ and $[Pd(en)(H_2O)_2]^{2+}$ with purine nucleosides and their 5′-monophosphates were studied in detail in the 1980s by Martin et al. [1,11], no systematic comparison with their behaviour towards the analogous 2′- and 3′-monophosphates appears to be available. This state of affairs is somewhat surprising in view of the potentiometric evidence presented by Sigel et al. for a significant degree of inner-sphere macrochela-

* Corresponding author. Tel.: +49-234-322 4192; fax: +49-234-321 4420

E-mail address: shel@anachem.ruhr-uni-bochum.de (W.S. Sheldrick).

0020-1693/02/$ - see front matter © 2002 Elsevier Science B.V. All rights reserved.
PII: S0020-1693(02)00921-0

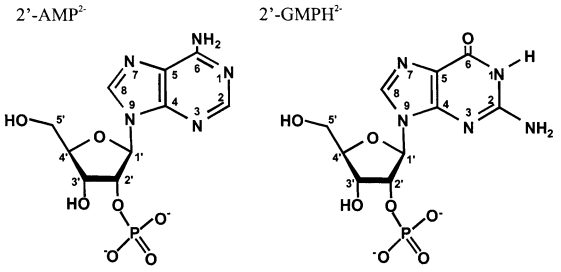

Scheme 1. 2′-AMP^{2-} and 2′-GMPH^{2-}.

tion in the Cu^{2+}/2′-AMP^{2-} and Cu^{2+}/2-GMP^{3-} equilibrium systems [12,13]. Despite its relatively low basicity, N3 binding is believed to be involved and spectroscopic support for this hypothesis has been provided by the recent NMR characterisation of a κ^3*N3,O*(ether),*O*(phosphate) Cu(PMEA) macrochelate (PMEA = 9-[2-(phosphonomethoxy)ethyl]adenine) [14]. N3 has also been confirmed through use of a repulsive energy methodology [15] as a sterically available coordination site for the interaction of (amine)Pt(II) fragments with purine nucleosides and X-ray structures with M–N3 binding have been reported for square planar Pt(II) and Rh(I) complexes of N9-substituted adenine and guanine derivatives [16–18]. We now present a comparative study using spectroscopic, potentiometric and chromatographic techniques of the interaction of (amine)M(II) fragments (amine = dien, en; M = Pd, Pt) with purine 2′- and 3′-nucleotides at metal-to-base ratios *R* between 1 and 3. Particular emphasis has been placed on the role of the phosphate site in facilitating specific metal fragment-nucleotide recognition through oligomer formation and/or inner/outer-sphere macrochelation [13,19].

2. Results

2.1. Interaction of $[Pd(dien)(H_2O)]^{2+}$ with purine 2′- and 3′-monophosphates

The equimolar (M:B molar ratio $R = 1$) equilibrium systems $[Pd(dien)(H_2O)]^{2+}$/*X*′-AMP^{2-} and $[Pd(dien)(H_2O)]^{2+}$/*X*′-GMP^{3-} (*X*′ = 2′ and 3′) were fully characterised by ^{1}H NMR pH titrations. Species were assigned on the basis of their pH and concentration (integral values for $R = 1$ and 2) dependence and by comparison with the literature values of Martin et al. [1] for the respective purine nucleoside 5′-monophosphates.

As illustrated in Fig. 1 for adenosine 2′-monophosphate (2′-AMP^{2-}) at pH* 3.14, the endocyclic nitrogens N1 and N7 are competitive Pd(II) coordination sites for adenine nucleotides. Mononuclear species $M_7BH_1H_P$/M_7BH_P/M_7B with N7 metal binding (M_7 designates N7 coordination, H_P phosphate protonation etc) can be assigned on the basis of their characteristic upfield ^{1}H NMR shifts in the pH* (pH meter values uncorrected for deuterium isotope effects in D_2O) range 2–4 of N1 deprotonation. A large displacement of the H2 and H8 resonances to higher field is also observed for the free nucleotide BH_2 on loss of its N1 proton (pK_a 3.74 [12]) and this step is compensated to a certain degree by a less pronounced downfield shift between pH* 5 and 7 due to the second phosphate deprotonation (pK_a 5.95 [12]). With the exception of BM_1H_P and BM_1, H8 resonances for individual species are all registered at markedly lower field than for the accompanying H2 signals. The contrasting H8/H2 shifts of the mononuclear N1-coordinated Pd(II) complexes were established by Martin et al. for the analogous 5′-AMP^{2-} species on the basis of H/D exchange experiments [1].

Fig. 2 depicts the pH* dependence of the added integral values for the H2 and H8 resonances of microspecies present in the $[Pd(dien)(H_2O)]^{2+}$/2′-AMP^{2-} equilibrium system for the range $3.0 \leq pH^* \leq 8.5$. The theoretical distribution curves for microspecies were calculated using results from a least-squares refinement of the individual log β values with the program NIBIP96 [20]. Stability constants log β for the macrospecies MBH, MB and M_2BH of 2′-AMP^{2-} were

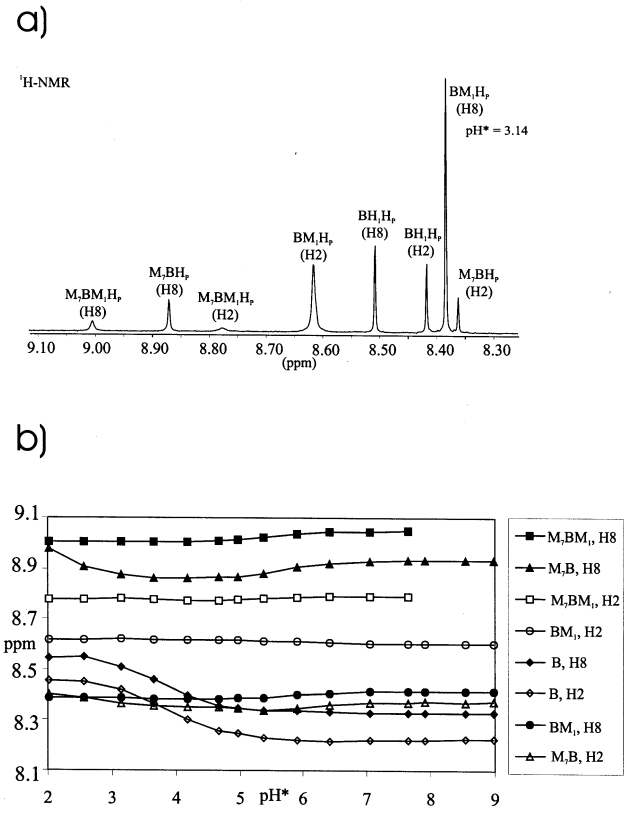

Fig. 1. (a) ^{1}H NMR spectrum for the equimolar (M:B, $R = 1$) aqueous equilibrium system $[Pd(dien)(H_2O)]^{2+}$/2′-AMPH$_2$ at pH* 3.14. The respective coordination and protonation sites in this and the following Figs. are given as lower indices; (b) pH* dependence of the adenine H2 and H8 NMR signals for species in the range $2 \leq pH^* \leq 9$.

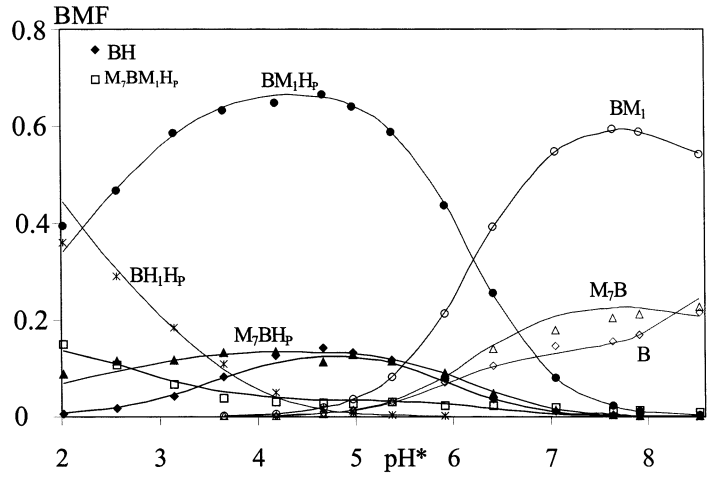

Fig. 2. Species distribution for the equimolar aqueous equilibrium system $[Pd(dien)(H_2O)]^{2+}$/2′-AMP^{2-} in the range $2 \leq pH^* \leq 8.5$ as established by ^1H NMR titration (BMF = fraction of the total nucleotide concentration).

also determined by a HYPERQUAD [21] analysis of potentiometric pH-titration data and are summarised in Table 1, together with the intrinsic log [N1/N7] binding ratios [1] for the microspecies BM_1/M_7B of the dianionic nucleotide and those for the phosphate protonated species BM_1H_P/M_7BH_P. A species distribution diagram very similar to that of the isomeric 2′-monophosphate in Fig. 2 is obtained for the $[Pd(dien)(H_2O)]^{2+}$/3′-AMP^{2-} equilibrium system. The absence of a specific intramolecular (dien)N–H···O (phosphate) hydrogen bonding interaction, as present in its N7-coordinated outer-sphere macrochelate with 5′-AMP^{2-}, leads to dominance of N1 binding for the (dien)Pd(II) fragment over the whole pH* range studied for 2′-AMP^{2-} and 3′-AMP^{2-}. In striking contrast, a crossover from N1 (in BM_1H_P/BM_1) to N7 preference (in M_7B) is observed for 5′-AMP^{2-} at pH 6.8 [1]. As may be gauged from the intrinsic log [N1/N7] binding ratios of −0.1 for the BM_1 and M_7B species of 5′-AMP^{2-}, the additional stabilisation of the N7 coordination mode due to outer-sphere macrochelation is just sufficient to outweigh the stronger basicity of N1. Protonation of the participating phosphate in BM_1H_P and M_7BH_P leads to a switch in the binding preference and an increase in the log [N1/N7] ratio to 0.4 [1]. The stronger basicity of N1 in comparison to N7 is clearly responsible for the dominance of N1-coordinated (dien)Pd(II) complexes in the distribution diagrams of 2′-AMP^{2-} (Fig. 2) and 3′-AMP^{2-}. A measure of the tendency of $[Pd(dien)(H_2O)]^{2+}$ to favour N1 over N7 is provided by the intrinsic log [N1/N7] binding ratios of 0.4/0.6 for the dianionic nucleotides (Scheme 2) and 0.6/0.7 for the respective monoprotonated phosphates.

Table 1
Experimental parameters for potentiometric and pH titration studies of the equilibrium systems formed between $[Pd(dien)(H_2O)]^{2+}$ and the purine nucleoside 2′-monophosphates, 2′-AMP^{2-} and 2′-GMP^{3-}

Nucleotide	2′-AMP^{2-}	2′-GMP^{3-}	2′-GMP^{3-}
1. Stability constants for macrospecies from potentiometric data			
M:B ratio R	1	1	3
C_M/mmol l^{-3}	1.0	1.0	3.0
C_B/mmol l^{-3}	1.0	1.0	1.0
I(electrolyte)/mol l^{-1}	0.1, KNO_3	0.1, KNO_3	0.1, KNO_3
pH range [a]	3.5–10.5	3.5–10.5	4.8–9.0
Temperature/K	298	298	298
Number of titrations	5	6	6
Number of data points	420	456	474
Goodness-of-fit S	1.9	2.5	3.5
log β(MBH_2)		20.82(3)	20.82 [b]
log β(MBH)	11.1(1)	15.40(4)	15.40 [b]
log β(MB)	5.30(4)	7.50(4)	7.50 [b]
log β(M_2BH)	13.5(1)	19.45 [b]	19.45(3)
log β(M_2B)		13.70 [b]	13.70(3)
log β(M_3B)		16.59 [b]	16.59(2)
2. Protonation constants from potentiometric data			
log β(BH_3)		17.97(2) [c]	
log β(BH_2)	9.69(2) [12]	15.57(2) [c]	
log β(BH)	5.95(1) [12]	9.62(1) [c]	
3. Intrinsic log [N1/N7] binding ratios from ^1H NMR data			
R value	0.041	0.008	
Log [β(BM_1H_P)/β(M_7BH_P)]	0.6		
Log [β(BM_1)/β(M_7B)]	0.4	0.3	

[a] practical pH scale (pH_{meas}) with $A = pH_{meas} - p[H]_{calc/conc} = 0.047(6)$ [27,28].
[b] Not refined.
[c] $C_B = 1$ mmol l^{-1}, pH range 2.0–11.5, 4 titrations, 445 data points.

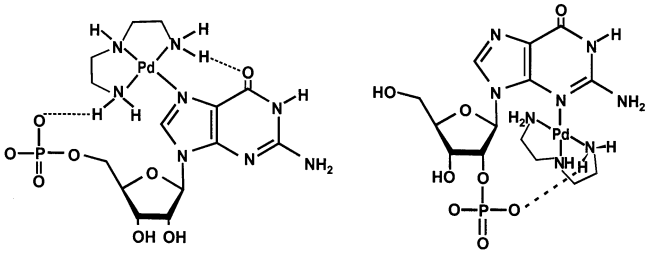

Scheme 2. $\kappa^2N7,O(P)$ and $\kappa^2N3,O(P)$ outer-sphere macrochelation for respectively 5′-$GMPH^{2-}$ and 2′-$GMPH^{2-}$.

The results of an analogous analysis of the interaction of $[Pd(dien)(H_2O)]^{2+}$ with the guanine nucleotide 2′-GMP^{3-} at $R = 1$ are also presented in Table 1. As depicted in Fig. 3b, H8 of the free diprotonated nucleotide BH_2 undergoes a small downfield displacement in the pH* range 5–7, owing to the second deprotonation of the phosphate group ($pK_{a2} = 5.95$), and this is followed by a more pronounced shift to higher field on N1 deprotonation ($pK_{a3} = 9.62$) in alkaline solution. The mononuclear N7-coordinated species M_7BH_1/M_7B can once again be assigned on the basis of the large displacement of their H8 resonance to lower field in comparison to the free nucleotide and by the characteristic upfield shift of this signal on N1 deprotonation. Microspecies distribution diagrams are very similar for 2′-GMP^{3-} (Fig. 4) and its 3′-isomer. As a result of the increased basicity of both N1 and N7 in guanine nucleotides, the concentration of dinuclear μ-N1, N7 bridged species ($M_7BM_1H_P/M_7BM_1$) is much higher for 2′- and 3′-GMP^{3-}, particularly in the range $6 \leq pH^* \leq 10$, than for the analogous adenosine 2′- and 3′-monophosphates. The absence of intramolecular (dien)N–H···O(phosphate) hydrogen bonding leads once again to a reversal of the intrinsic log [N1/N7] binding ratio, in this case from −0.2 for 5′-GMP^{3-} [1] to respectively 0.3 and 0.4 for BM_1/M_7B species of 2′-GMP^{3-} and 3′-GMP^{3-}. As a result, a crossover from N7 to N1 preference is observed in alkaline solution for these nucleotides, in contrast to 5′-GMP^{3-}, e.g. at pH* 8.3 for 2′-GMP^{3-} from M_7BH_1/M_7B to BM_1.

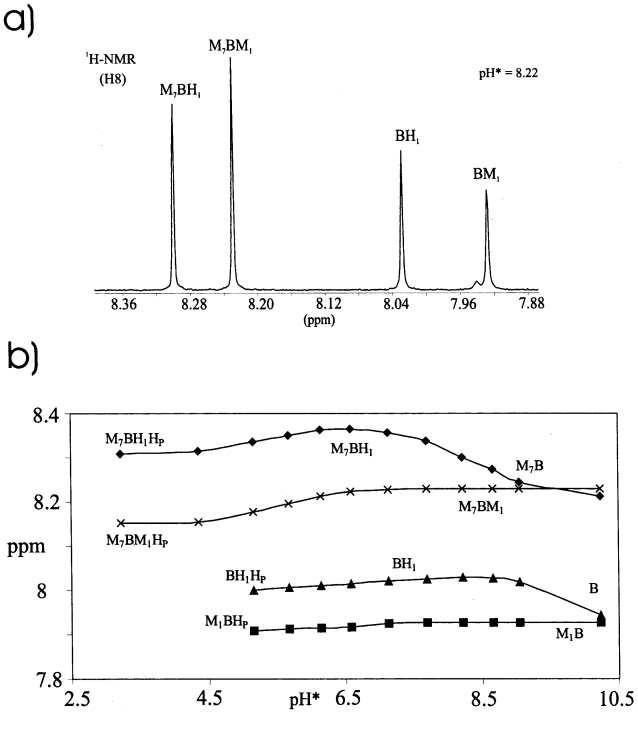

Fig. 3. (a) ^{1}H NMR spectrum for the equimolar (M:B, $R = 1$) aqueous equilibrium system $[Pd(dien)(H_2O)]^{2+}$/2′-$GMPH^{2-}$ at pH* 8.22; (b) pH* dependence of the guanine H8 NMR signal for species in the range $3.2 \leq pH^* \leq 10.2$.

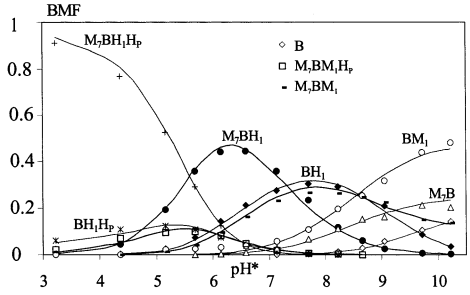

Fig. 4. Species distribution for the equimolar aqueous equilibrium system $[Pd(dien)(H_2O)]^{2+}$/2′-GMP^{3-} in the range $3.2 \leq pH^* \leq 10.2$ as established by ^{1}H NMR titration (BMF = fraction of the total nucleotide concentration).

Fig. 5 depicts the ^{1}H NMR spectrum of a 3:1 $[Pd(dien)(H_2O)]^{2+}$/2′-AMP^{2-} equilibrium system at pH* 6 and illustrates how the mononuclear N1-coordinated species BM_1/BM_1H_P is competitive with the dinuclear μ-N1, N7 bridged complex $M_7BM_1H_P/M_7BM_1$ for adenine nucleotides even for a large $[Pd(dien)(H_2O)]^{2+}$ excess. Although comparison of this spectrum with that for $R = 1$ in Fig. 1a confirms the presence of new signals, presumably due to O(phosphate)-coordinated complexes, these evidently belong to minor species. Threefold metallation of the adenine base at N1, N3 and N7 would be expected to lead to resonances at markedly lower field than for $M_7BM_1H_P/M_7BM_1$ at δ 9.07 and Fig. 5 clearly provides no evidence for the presence of such species in an $R = 3$ solution at pH* 6.0.

This coordination behaviour of 2′-AMP^{2-} (and 3′-AMP^{2-}) is in striking contrast to that of the analogous guanosine 2′-monophosphate, for which selected ^{1}H and ^{31}P NMR spectra for solutions with a threefold $[Pd(dien)(H_2O)]^{2+}$ excess are presented in Fig. 6. In addition to the signals 2 and 3 of the species $M_7BM_1H_P$ and $M_7BH_1H_P$, which are also present at $R = 1$ (Fig. 4), three new resonances in the ^{1}H NMR spectrum at pH* 4.18 can be assigned respectively to two O(phosphate)-coordinated species $BM_1M_PH_P$ (**1**) and $M_7BM_PH_1$ (**4**) and the trinuclear μ_3-N1,N3,N7 bridged complex $M_7BM_1M_3$ (**5**). The guanine metal binding sites in $BM_1M_PH_P$ and $M_7BM_PH_1$ are indicated by the opposite upfield (δ 7.95) and downfield shifts (δ 8.46) of the H8 resonance with respect to that of the free nucleotide. Trimetallation of the purine base in $M_7BM_1M_3$ leads to a marked displacement to lower field and the appearance of rotamer doublets at δ 8.78 and 8.96. Following deprotonation of the second phosphate, the ^{1}H NMR spectrum at pH* 6.48 displays increased concentrations of $BM_1M_PH_P$ (**1**) and $M_7BM_PH_1$ (**4**) and also includes a second trimetallated complex $M_7BM_1M_P$ (**6**). Direct O(phosphate) coordination in these species is confirmed

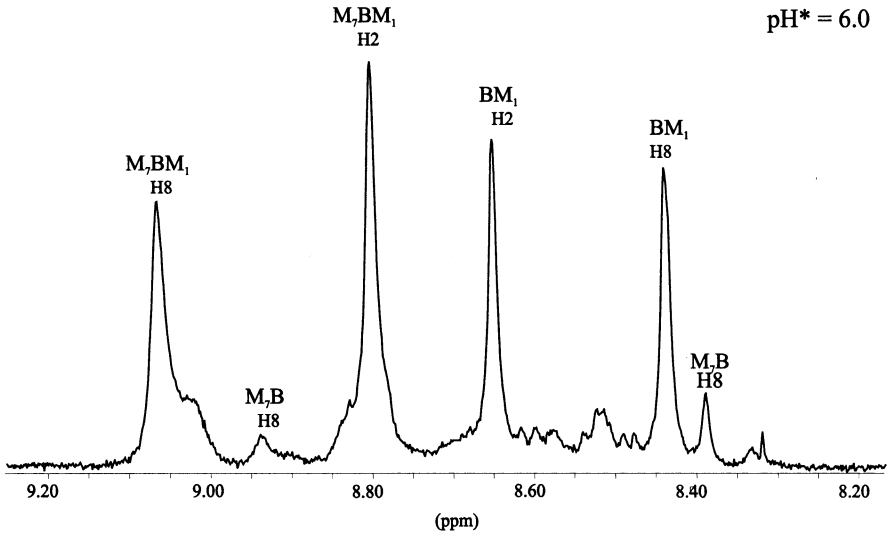

Fig. 5. ^{1}H NMR spectrum for the aqueous equilibrium system $[Pd(dien)(H_2O)]^{2+}$/2′-AMP^{2-} at pH* 6.0 and $R = 3$ (M:B).

by the observation of a ^{31}P NMR resonance at approximately 5 ppm to lower field in comparison to the solely base coordinated complexes M_7BM_1, M_7BH_1 and $M_7BM_1M_3$ (2, 3 and 5). At high pH* (8.54) the μ-N1, N7 bridged complex M_7BM_1 predominates and a signal for 2′-$GMPH^{2-}$ (**7**) itself can be observed. A comparison of the pH* dependence of mono-, di- and trinuclear macrospecies in the $[Pd(dien)(H_2O)]^{2+}$/2′-GMP^{3-} equilibrium system at $R = 3$, as determined on the basis of potentiometric titrations (Fig. 7), provides support for the correctness of the above assignments. It is apparent that trinuclear species including $M_7BM_1M_3$ exhibit their maximum concentration in the pH* range 6.0–7.5.

It is particularly interesting to compare ^{1}H NMR spectra for the three guanosine monophosphates at this M:B ratio (Fig. 8), as these demonstrate the importance of intramolecular (dien)N–H···O(phosphate) hydrogen bonding for the relative stability of the various di- and trinuclear species. For 5′-$GMPH^{2-}$ (pH* 7.1) outer-sphere macrochelation involving the N7 binding site leads to a dramatic stabilisation of the dinuclear species M_7BM_1, which is accompanied by a marked downfield displacement of the H8 resonance in comparison to the analogous 2′- and 3′-$GMPH^{2-}$ complexes. As a result, the O(phosphate)- coordinated species BM_1M_P and $M_7BM_1M_P$ are only of minor importance for 5′-$GMPH^{2-}$ and both M_7BH_1 and $M_7BM_PH_1$ cannot even be detected at pH* 7.1. Intramolecular (dien)N–H···O(phosphate) hydrogen bonding is sterically unfavourable for all three potential guanine binding sites N1, N3 and N7 in 3′-GMP^{3-} complexes and this is reflected in a marked increase in direct O(phosphate) binding in comparison to the 5′-nucleotide. Mainly responsible for the apposite resonances in the ^{31}P NMR spectrum of the $[Pd(dien)(H_2O)_2]^{2+}$/3′-GMP^{3-} equilibrium system ($R = 3$) is species $M_7BM_1M_P$, whose ^{1}H signal coincides with that of M_7BM_1. In contrast, the proximity of the phosphate group to N3 in 2′-GMP^{3-} suggests that outer-sphere macrochelation of (dien)Pd(II) involving these coordination/hydrogen bonding sites should be sterically favourable. The ^{1}H NMR spectrum of Fig. 8a indicates that this must, indeed, be the case. For instance, intramolecular (dien)N–H···N3 hydrogen bonding from a 2′-phosphate coordinated (dien)Pd(II) fragment may be responsible for the relative increase in the concentration of $M_7BM_PH_1$ in comparison to 3′-GMP^{3-} and 5′-GMP^{3-}. More importantly, the dramatic increase in the stability of the trimetallated species $M_7BM_1M_3$ for 2′-GMP^{3-} may be assumed to result from an outer-sphere macrochelation involving (dien)N–H···O(phosphate) hydrogen bonds from an adjacent N3-coordinated (dien)Pd(II) fragment. As a result, this species represents approximately 20% of the total base concentration in comparison to only approximately 4% for 3′-GMP^{3-} and approximately 8% for 5′-GMP^{3-}. The presence of *anti* and *syn* rotamers relative to the 2-amino group (Fig. 9) causes a splitting of the $M_7BM_1M_3$ H8 resonances for all three nucleotides. The doubling of the number of rotamers for 2′-GMP^{3-} and 5′-GMP^{3-} is presumably due to hindered rotation between two favoured nucleotide conformations at the glycosidic bond N9–C1′. The observation of preferred μ-N1, N3, N7 trimetallation for 2′-GMP^{3-} suggests that both outer- and inner-sphere $\kappa^2 N3,O$(phosphate) coordination should be possible for bidentate fragments such as (en)Pd(II) and (en)Pt(II).

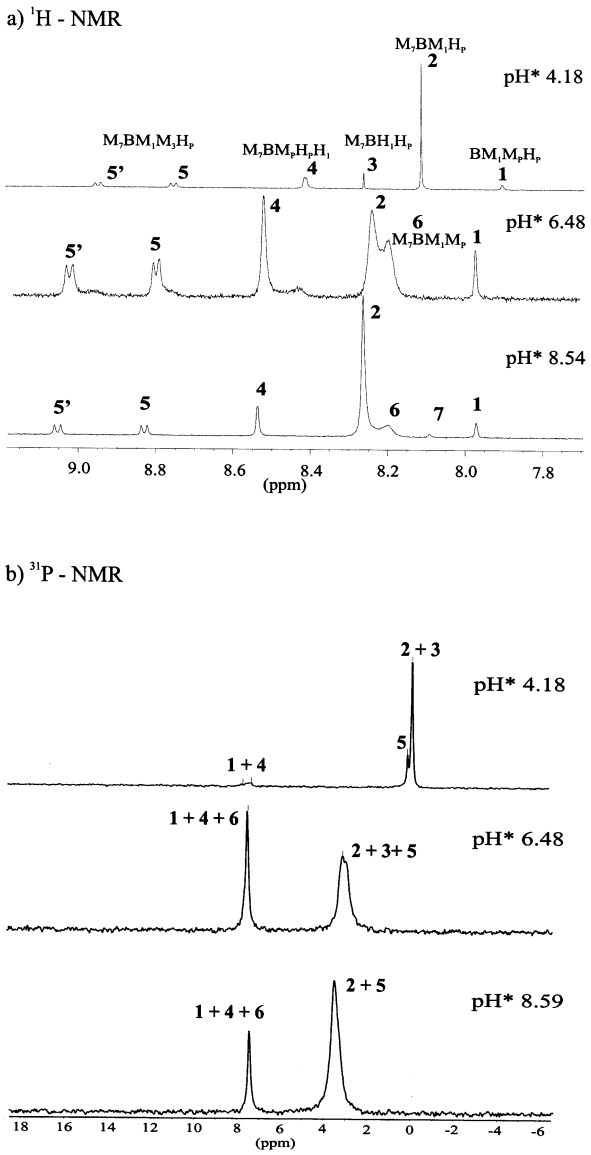

Fig. 6. (a) ^{1}H NMR spectra for the aqueous equilibrium system $[Pd(dien)(H_2O)]^{2+}$/2′-GMP^{3-} at $R = 3$ (M:B) and selected pH* values; (b) ^{31}P NMR spectra for the same system at the selected pH* values.

2.2. Interaction of $[Pd(en)(H_2O)_2]^{2+}$ with 2′-GMP^{3-} and 5′-GMP^{3-}

Although the pH-dependent interaction of the potentially bidentate fragment $(en)Pd^{2+}$ with 5′-GMP^{3-} has been studied in detail using NMR, Raman, IR and CD spectroscopy [3,5,11], no binding constants appear to have been previously reported for the major species MB_2H_x ($x = 4$, 2, 0) and MBH_x ($x = 1$, 0). For comparison purposes, we have, therefore, included the $[Pd(en)(H_2O)_2]^{2+}$/5′-GMP^{3-} equilibrium system in our current studies and experimental parameters based on a least-squares fit to potentiometric pH-titration data (at $R = 0.5$) are listed for both the 2′- and 5′-nucleotide in

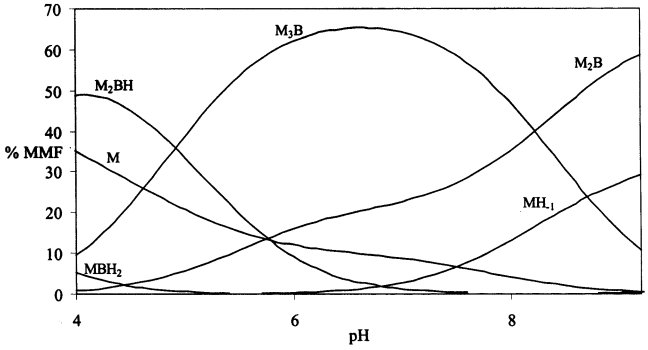

Fig. 7. pH* dependence of macrospecies present in the $[Pd(dien)(H_2O)]^{2+}$/2′-GMP^{3-} equilibrium system at $R = 3$ as determined by potentiometric titration. The concentrations are given as mole percentages of the total metal ion concentration (% MMF).

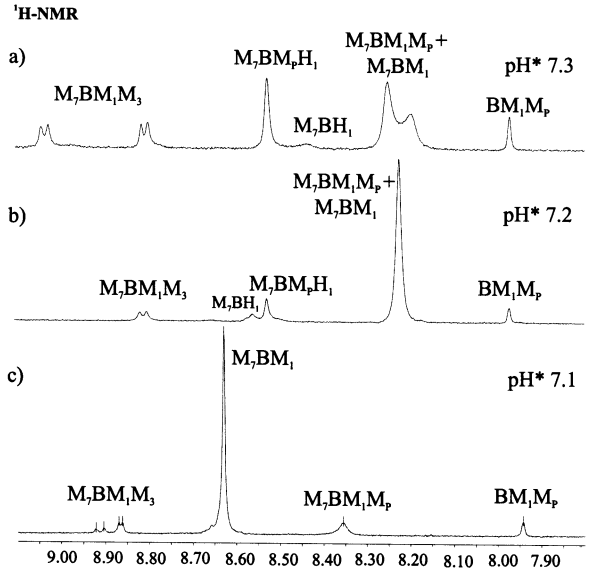

Fig. 8. ^{1}H NMR spectra for the given $[Pd(dien)(H_2O)]^{2+}$/X′-$GMPH^{2-}$ equilibrium system at $R = 3$ (M:B): (a) 2′-$GMPH^{2-}$ at pH* 7.3; (b) 3′-$GMPH^{2-}$ at pH* 7.2; and (c) 5′-$GMPH^{2-}$ at pH* 7.1.

Table 2. As illustrated in Fig. 10b, only three species are present in the 1:2 reaction mixture of $[Pd(en)(H_2O)_2]^{2+}$ and 5′-$GMPH^{2-}$ at pH* 7.01, namely the N7-coordinated complex $[Pd(en)(5'\text{-GMPH-}\kappa N7)_2]^{2-}$ (MB_2H_2), the μ-*N1*,*N7* bridged oligomer $[\{Pd(en)(5'\text{-GMPH-}\mu\text{-}N1,N7)\}]_n$ (MBH/MB) and the free 5′-nucleotide (BH). ^{1}H $\{^{15}N\}$ NMR shifts together with $^{31}P\{^1H\}$ NOEs have confirmed outer-sphere macrochelation involving intramolecular (en)N–H···O(phosphate) hydrogen bonding for the dianionic MB_2H_2 (pH 7) and neutral species MB_2H_4 (pH 2–3) in solution [5]. Both ^{31}P NMR and Raman bond shifts suggest that an analogous interaction must also be responsible for stabilising the μ-N1, N7 bridged oligomer MBH/MB [3]. A cyclic tetrameric structure with idealised C_4 symmetry for the participating purine bases was proposed for this complex by Uchida et al. [3] on the basis of their ^{1}H NMR studies on mixed 5′-GMP^{3-}/5′-IMP^{3-} species [3].

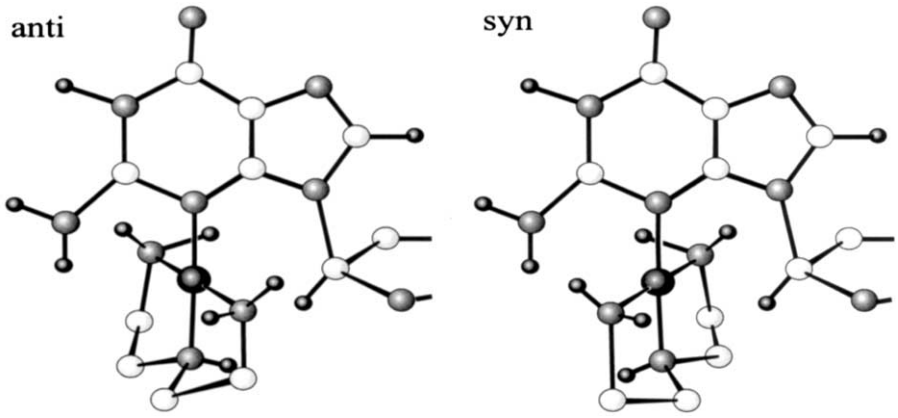

Fig. 9. Possible *anti* and *syn* configurations of the N3-coordinated (dien)Pd(II) fragment relative to the 2-amino group in complexes of guanosine monophosphates.

Table 2
Experimental parameters for potentiometric studies of the equilibrium systems formed between $[Pd(en)(H_2O)_2]^{2+}$ and the guanine nucleotides, 2′-GMP^{3-} and 5′-GMP^{3-}

Nucleotide	2′-GMP^{3-}	5′-GMP^{3-}
M:B ratio R	0.5	0.5
C_M/mmol l^{-3}	0.5	0.5
C_B/mmol l^{-3}	1.0	1.0
I(electrolyte)/mol l^{-3}	0.1, KNO_3	0.1, KNO_3
pH range [a]	3.5–10.3	2.0–10.5
Temperature/K	298	298
Number of titrations	7	13
Number of data points	422	819
Goodness-of-fit S	2.8	–
R value	–	1.33 [b]
log β(MB_2H_4)	39.57(3)	40.96(7)
log β(MB_2H_2)	28.4(2)	28.8(1)
log β(MB_2)	13.52(3)	11.7(1)
log β(MBH)	15.98(3) [c]	16.37(5) [d]
log β(MB)	9.54(3) [c]	9.83(5) [d]

[a] practical pH scale (pH_{meas}) with $A = pH_{meas} - p[H]_{calc/conc} = 0.047(6)$ [27,28].
[b] protonation constants from potentiometric data ($I = 0.1$ mol l^{-1}, $T = 298$ K): pK_a(BH) 9.49(1), $pK_a(BH_2)$ 6.25(2), $pK_a(BH_3)$ 2.48(4) [19].
[c] present in solution as mixture of oligomers $M_xB_yH_z$ and M_xB_y.
[d] present in solution as cyclic tetramers $M_4B_4H_4$ amd M_4B_4.

We have confirmed the proposed nuclearity ($n = 4$) for the cyclic oligomer by mass spectrometry. At pH 8.3, a negative ion ESI mass spectrum contains molecular ions at m/z 1054.3, 703.1 and 526.2, whose $\Delta m/z$ values allow their assignment to $[M_4B_4H_2]^{2-}$ [($\Delta m/z = 0.5$), $[M_4B_4H]^{3-}$ [($\Delta m/z = 0.33$) and $[MB]^{-}$ ($\Delta m/z = 1.0$). The registration of the first two peaks provides unequivocal evidence for the presence of a tetranuclear complex in solution. A time dependent ^{1}H NMR study at pH* 6.5 and $T = 298$K (Fig. 11a) indicates that, following initial rapid formation of the κ^2N7, $N7'$ coordinated species MB_2H_4/MB_2H_2, construction of the μ-*N1, N7* bridged tetranuclear complex $M_4B_4H_4$/M_4H_4 is relatively slow. The absence of additional ^{1}H NMR signals during the course of this assembly process suggests that ring formation may be achieved by N1 metallation of two MB_2H_4 /MB_2H_2 species through subsequently linking (en)Pd^{2+} fragments. This reaction pathway would lead to a tetranuclear complex with alternating κ^2N7, $N7'$ and κ^2N1, $N1'$ coordination of the (en)Pd^{2+} fragments (Fig. 11b) rather than the C_4 symmetric tetramer with solely κ^2N7, $N1'$ coordination proposed by Uchida et al. [3]. Molecular modeling suggests that such a coordination mode should indeed be possible.

Our time dependent ^{1}H NMR and potentiometric studies indicate that, though relatively slow, equilibrium achievement is still rapid enough to allow satisfactory pH titrations for $[Pd(en)(H_2O)_2]^{2+}$/guanine nucleotide reaction mixtures. A model involving MB_2H_4/MB_2H_2, MBH/MB and MB_2 provides good least-squares fits to the experimental potentiometric data for both 2′-GMP^{3-} and 5′-GMP^{3-} (Table 2). However, in contrast to the latter nucleotide, the ^{1}H NMR data presented in Fig. 10a for 2′-GMP^{3-} indicate the presence of a large number of μ-*N1*, *N7* bridged oligomeric complexes (δ 8.1–8.7) of presumably differing nuclearities and conformations in the pH* range 5.5–9.5. Similar ^{1}H NMR spectra are obtained for the $[Pd(en)(H_2O)_2]^{2+}$/3′-GMP^{3-} reaction system. This striking lack of specific complex formation in comparison to 5′-GMP^{3-} with its characteristic cyclic tetranuclear species may once again be explained by the absence of stabilising intramolecular (en)N–H···O(phosphate) interactions for 2′-GMP^{3-} complexes formed at $R \leq 1.0$. The contribution of this outer-sphere macrochelation to the stability constant for the κ^2N7, $N7'$ coordinated 5′-$GMPH_2^-$ complex MB_2H_4 can be gauged by comparing its log β(MB_2H_4) value of 40.96(7) to that of 39.57(3) for the analogous 2′-$GMPH_2^-$ species (Table 2). It is also apparent from Table 2 that the 1: 1 species MBH/MB must provide an adequate average model (i.e. $x = y$) for the oligomeric

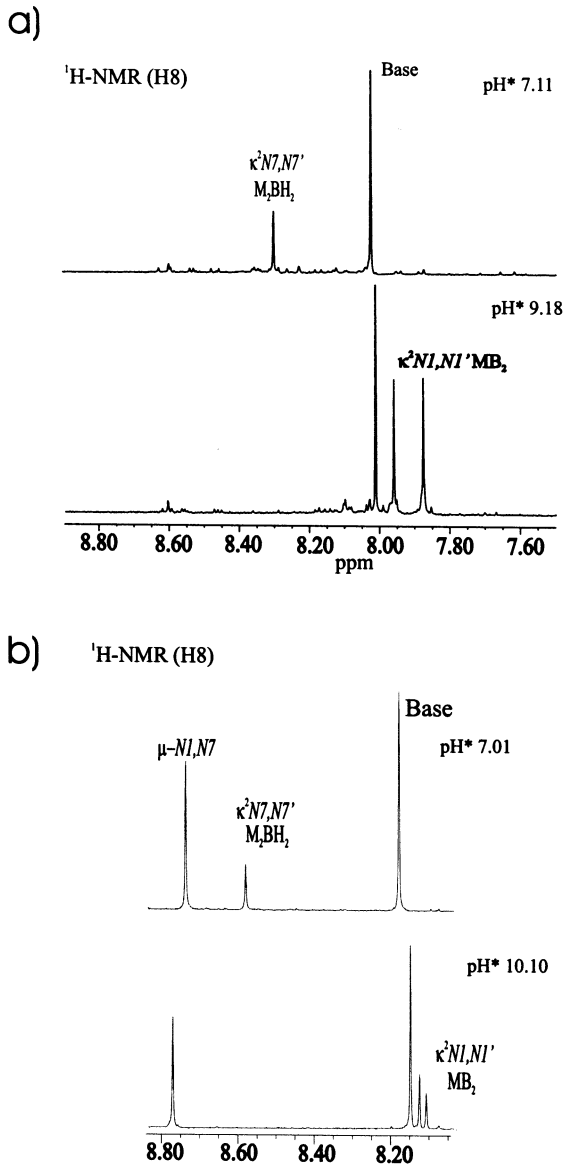

Fig. 10. Comparison of the ^{1}H NMR spectra for the $[Pd(en)(H_2O)_2]^{2+}$/X′-$GMPH^{2-}$ equilibrium systems at $R = 0.5$ (M:B): (a) 2′-$GMPH^{2-}$ at pH* 7.11 and 9.18; (b) 5′-$GMPH^{2-}$ at pH* 7.01 and 10.10.

complexes $M_xB_yH_z/M_xB_y$ present in the $[Pd(en)(H_2O)_2]^{2+}$/2′-GMP^{3-} equilibrium system at pH* > 5. This finding is confirmed by the ^{1}H NMR species distribution diagram depicted in Fig. 12, in which the sum of the integral values for oligomer resonances is assigned to MBH/MB. Further support for this approach is also provided by the negative ion ESI mass spectrum for a solution with $R = 2$ (0.5 mM 2′-$GMPH^{2-}$) at pH 7.29. This contains peaks at m/z 361.9, 888.9 and 1054.7 that can be assigned to respectively $[B+2H]^-$, $[MB_2H_3]^-$ and $[M_2B_2H]^-$ + $[M_4B_4H_2]^{2-}$ on the basis of their isotopic patterns and $\Delta m/z$ values. In contrast to the 2′-GMP^{3-} equilibrium system, the μ-N1,N7 bridged oligomer (as a tetranuclear species) is predominant over the whole pH* range 6.7–9.5 for 5′-GMP^{3-}.

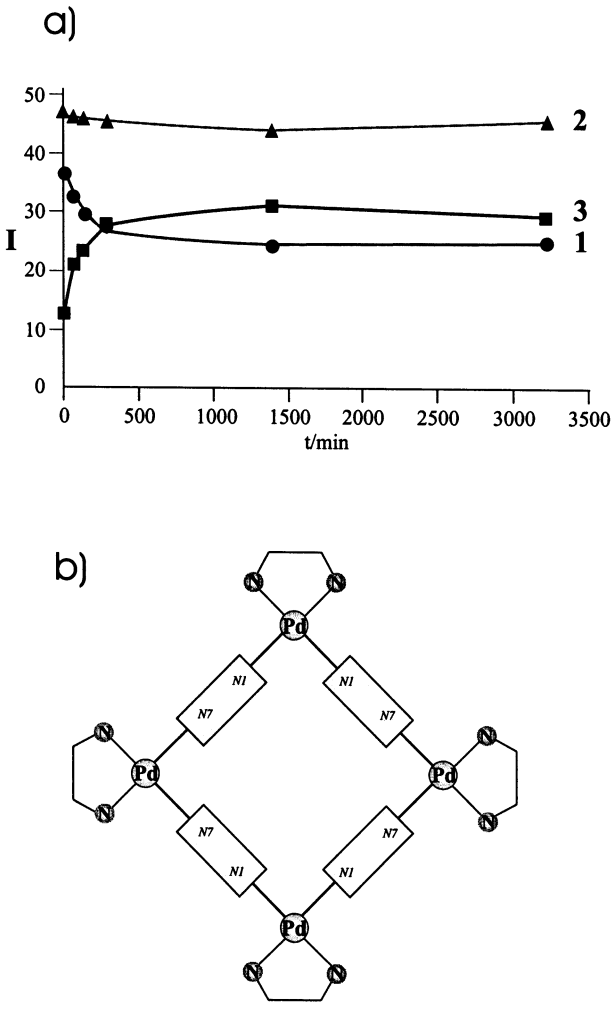

Fig. 11. (a) Time dependence of the ^{1}H NMR signal integrals for the reaction system $[Pd(en)(H_2O)_2]^{2+}$/5′-$GMPH^{2-}$ at pH* 6.5, $T = 298$ K: **1** = MB_2H_2, **2** = BH, **3** = M_4B_4; (b) Schematic representation of the alternating $\kappa^2N7,N7'$ and $\kappa^2N1,N1'$ coordination pattern in the tetramer M_4B_4 (**3**).

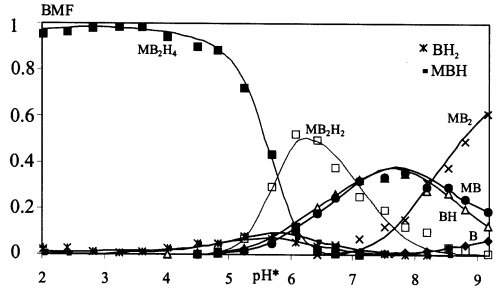

Fig. 12. Species distribution for the aqueous equilibrium system $[Pd(en)(H_2O)_2]^{2+}$/2′-GMP^{3-} at $R = 0.5$ as established by ^{1}H NMR titration for the range $2 \le pH^* \le 9.2$.

As for the monodentate fragment (dien)Pd^{2+}, 2′-GMP^{3-} and 3′-GMP^{3-} exhibit a contrasting coordination behaviour in the presence of a $[Pd(en)(H_2O)_2]^{2+}$ excess. Whereas the ^1H NMR spectra for the $[Pd(en)(H_2O)_2]^{2+}$/2′-$GMPH_2^-$ reaction system at $R = 2$ in the range $2 \leq pH^* \leq 6$ provide clear evidence for trimetallation (N1, N3, N7) of the guanine base due to the presence of a number of resonances in the δ range 9.1–10.1, this is not the case for 3′-$GMPH_2^-$. In this case no resonances above δ 8.8 could be detected.

2.3. Addition of $[Pt(en)(H_2O)_2]^{2+}$ to $[Pt(dien)(H_2O)]^{2+}$/X′-GMP^{3-} (X = 2′, 3′ and 5′) equilibrium systems at $R = 2.5$

The presence of numerous μ-N1,N7 bridged oligomers prevents a detailed ^1H NMR species analysis for the $[Pd(en)(H_2O)_2]^{2+}$/2′-GMP^{3-} equilibrium system at $R = 2$. This finding prompted us to follow an alternative strategy of blocking both N1 and N7 with (dien)Pt(II) fragments, whose relative kinetic inertness towards substitution in the resulting dinuclear complex $[\{Pt(dien)\}_2$(2′-GMP-μ-*N1*, *N7*)$]^+$, then allows a systematic study of the coordination of bidentate (en)Pt(II) by the remaining potential donor atoms, N3 and/or the phosphate O atoms. As this species M_7BM_1 slowly equilibrates to a mixture of itself and M_7B in aqueous solution, following separation by reversed phase HPLC, all investigations were performed on the $[Pt(dien)(H_2O)]^{2+}$/2′-GMP^{3-} equilibrium system at $R = 2.5$. After standing for 24 h, such a solution contains solely M_7BM_1 (signal **1**) and $M_7BM_1M_3$ (signal **3**) in a approximately 85:15 ratio (pH* 7.5). Following subsequent addition of an equivalent of $[Pt(en)H_2O)_2]^{2+}$, four new sets of ^1H NMR signals **4**–**7** are apparent after 300 h (Fig. 13a), that can be assigned to respectively $M_7BM_1M_P$(en), M_7BM_P(en)H_1, $M_7BM_1M_{3,P}$(en)*i-s* and $M_7BM_1M_3$(en)*o-s*. Due to the concomitant reduction in pH* to 6.3, the mononuclear complex M_7BH_1 (signal **2**) can also be observed in the equilibrium mixture as a minor species with δ 8.62. The pronounced downfield shifts of signals **6** (δ 9.54) and **7** (δ 10.14) with respect to $M_7BM_1M_3$(dien) (signal **3**, δ 9.35) suggest that these must also belong to trimetallated species, in this case the inner- and outer-sphere κ^2N3,O(phosphate) macrochelates $M_7BM_1M_{3,P}$(en)*i-s* and $M_7BM_1M_3$(en)*o-s*.

As depicted in Fig. 14, species **7**, **7**′ are formed rapidly through (en)Pt(II) coordination by N3 of the dinuclear complex **1** and reach a concentration maximum after approximately 24 h. Initially two distinct sets of ^1H NMR signals can be observed for such $M_7BM_1M_3$(en)*o-s* species at δ 10.08(**7**′) and 10.14(**7**), the former of which slowly wane in intensity as the concentration of the second trimetallated complex (signal **6**) increases. On reaching equilibrium after approximately 300 h, only the doublet at δ 10.14 belonging to **7** remains (Fig. 13a). These observations lead us to propose respectively outer- and inner-sphere κ^2N3,O(phosphate) binding modes for the (en)Pt(II) fragment in species **7**, **7**′ and **6**. Of the two initial rotamers **7**′ and **7** (see Fig. 15) of $M_7BM_1M_3$(en)*o-s*, which are formed in similar concentrations, only **7**′, with its water ligand on the same side of the guanine base as the 2′-phosphate function, can allow direct reaction to the inner-sphere macrochelate **6** (see Fig. 16). These signal assignments provide a satisfactory explanation for both the accompanying decrease in intensity for the ^1H NMR signal of **7**′ as **6** gains in strength and the fact that **7** and **6** are present in similar concentrations in the final reaction solution. The ethylenediamine chelate ring in **7** can adopt either a λ or δ configuration and their individual stabilisation through intramolecular N–H···O(phosphate) hydrogen bonding can be assumed to be responsible for the observation of two resonances for this $M_7BM_1M_3$-(en)*o-s* species in Fig. 13a. Formation of a direct Pt–O bond in the inner-sphere macrochelate **6** leads to charge reduction at the metal centre, that is accompanied by a marked upfield shift for the guanine H8 ^1H NMR signal.

Marzilli et al. have demonstrated how addition of an excess of NaCl to the κ^2N7,O(phosphate) macrochelate $[cis$-$Pt(ND_2CH_3)_2$(5′-ATP-$\kappa^2N7,O_\gamma)]^{2-}$ leads to an equilibrium mixture of this original complex and $[cis$-$PtCl(ND_2CH_3)_2$(5′-ATPH-$\kappa N7)]^{2-}$ [22]. Fig. 13b depicts the ^1H NMR spectrum taken for the (dien)Pt(II)/(en)Pt(II)/2′-GMP^{3-} equilibrium mixture following its analogous incubation with a 100-fold excess of KCl for 24 h at 313 K. Interestingly, whereas the concentration of the inner-sphere κ^2N3,O(phosphate) macrochelate **6** remains effectively unchanged, partial substitution of the remaining water ligand in **7** by Cl^- does lead to the appearance of the expected third trimetallated species $M_7BM_1M_{3,Cl}$(en) **8** at δ 9.97. Its doublets may once again be assumed to be due to stabilisation of λ or δ chelate ring configurations by intramolecular (phosphate)O···H–N bonding. As previously, the downfield shift relative to **7** can be ascribed to charge reduction at the metal centre of the coordinated (en)Pt(II) fragment. Similar resonances are observed for the reaction of *cis*-$[PtCl_2(NH_3)_2]$ with the $[Pt(dien)(H_2O)]^{2+}$/2′-GMP^{3-} equilibrium system at $R = 2.5$. The optimised structures of theoretical mononuclear inner- and outer-sphere κ^2N3,O(phosphate) complexes of the $(NH_3)_2$Pt(II) fragment are depicted in Fig. 15 and were calculated with the program AMBER (Hyperchem) using the force field parameters of Marzilli et. al [23].

In stark contrast to 2′-GMP^{3-} (Fig. 13a), no characteristic downfield signals for direct phosphate binding can observed in the ^{31}P NMR spectrum of an analogous (dien)Pt(II)/(en) Pt(II)/3′-GMP^{3-} reaction mixture after 300 h. Although the presence of species $M_7B_1M_PH_1$ does lead to the appearance of a single

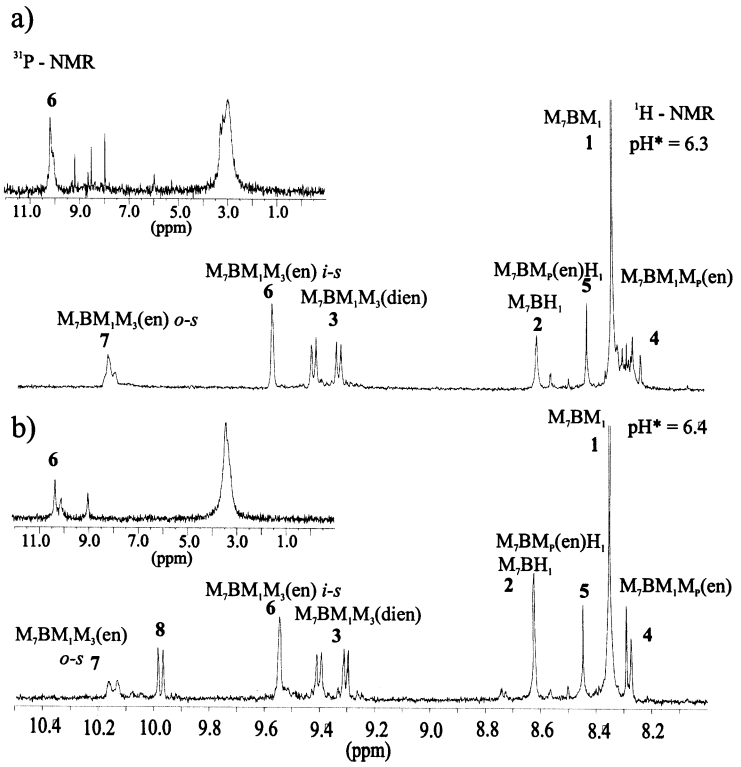

Fig. 13. ^{1}H and ^{31}P NMR spectra of the aqueous reaction system $[Pt(dien)(H_2O)]^{2+}$/2′-GMPH^{2-} ($R = 2.5$): (a) following reaction (300 h) with $[Pt(en)(H_2O)_2]^{2+}$ ($R = 1.0$) at 295 K; and (b) 24 h after incubation of the resulting solution with KCl ($R = 100$) at 313 K.

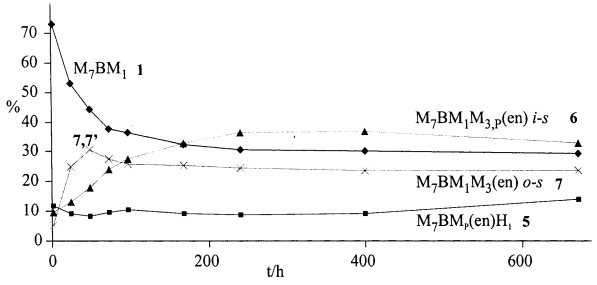

Fig. 14. Time dependence of the integral values of signals **1**, **5**, **6** and **7**, **7**′ during the course of the reaction of $[Pt(dien)(H_2O)]^{2+}$/2′-GMPH^{2-} ($R = 2.5$) with $[Pt(en)(H_2O)_2]^{2+}$ ($R = 1.0$) at 295 K.

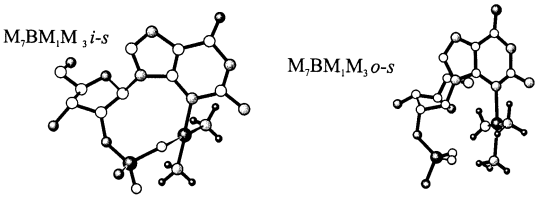

Fig. 15. Optimised force field structures (AMBER) for theoretical mononuclear inner- and outer-sphere κ^2N3,O(phosphate) complexes of the $(NH_3)_2$Pt(II) fragment with 2′-GMPH^{2-}. The Pt(II) atoms exhibit an N3 binding mode analogous to that of species **6** and **7**.

resonance at δ 8.3 in the case of 5′-GMP^{3-}, its Pt–O(phosphate) interaction is only of minor importance for the 5′-nucleotide. This state of affairs is also reflected

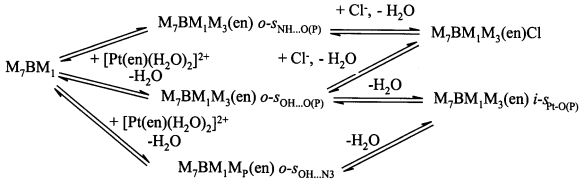

Fig. 16. Proposed reaction pathways for the formation of the inner-sphere κ^2N3, O(phosphate) macrochelate **6**.

in the reversed phase HPLC traces obtained for (dien)Pt(II)/(en)Pt(II)/X′-GMP^{3-} reaction mixtures after 300 h (Fig. 17). Fractions 1 and 2 are observed for all three guanine nucleotides and can safely be assigned to species of the types M_7BM_1 and $M_7BM_1M_3$(dien), all of which exhibit characteristic UV absorption maxima in the range 230–240nm, as does the unique fraction 3 for 2′-GMP^{3-}. In contrast, such an absorption band is missing for fraction 4 and the similarity of its UV spectrum to that of M_7BH_1 indicates that it may contain $M_7BM_P(en)H_1$ (species **5** in Fig. 13a). Following semi-preparative reversed phase HPLC in the presence of the ion pairing agent pentafluoropropionic acid (PFP), the contents of fractions 2 and 3 for 2′-GMP^{3-} were characterised by NMR and FAB mass spectrometry.

The assignment to $M_7BM_1M_3$(dien) is confirmed for the former fraction by the presence of characteristic doublets at δ 9.38 and 9.48 in its ^{1}H NMR spectrum at

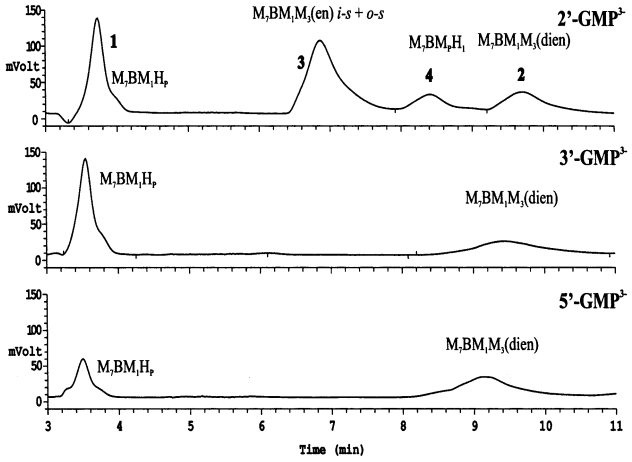

Fig. 17. Comparison of reversed phase chromatograms for reaction solutions $[[Pt(dien)(H_2O)]^{2+}/[Pt(en)(H_2O)_2]^{2+}/X'\text{-}GMP^{3-}$ ($R = 2.5/1.5$, $x = 2$, 3, 5) after 300 h (eluent H_2O/CH_3OH at 83:17 ratio with 0.1% PFP).

pH* 2.0 (Fig. 18b). This also includes a singlet at δ 8.64 belonging to $M_7BH_1H_P$, which is presumably formed by cleavage of the Pt–O(phosphate) bond of $M_7BM_P(en)H_1$ (from the neighbouring fraction 4) under the strongly acid conditions (pH* 2.0) required for HPLC separation in the presence of the ion pairing agent PFP. Fraction 3 contains both the inner- and outer-sphere κ^2N3,O(phosphate) macrochelates **6** and **7** and direct Pt–O binding is confirmed for the former complex by the presence of a strong downfield ^{31}P NMR singulet at δ 7.8 (Fig. 18a) The second $M_7BM_1M_3(en)$*o-s* resonance set at δ 9.73 (signal **8′**) is presumably due to partial substitution of the original water ligand in **7** by the $CF_3CF_2COO^-$ anion of the HPLC ion pairing agent PFP. As also observed for fraction 2, a small quantity of $M_7BH_1H_P$ from the central fraction 4 is present as a contamination. The FAB mass spectrum of fraction 3 exhibits molecular ion peaks at *m/z* 1210, 1374, 1538 and 1702 belonging to $[\{Pt(dien)\}_2Pt(en)(2'\text{-}GMP)+2H]^+ = M^+$, $[M+PFP]^+$, $[M+2PFP]^+$ and $[M+3PFP]^+$. No molecular ions for oligomeric species are observed, thereby providing confirmation that $M_7BM_1M_{3,P}$(en)*i-s* (**6**) is indeed a κ^2N3,O(phosphate) macrochelate and not a dimer or species of higher nuclearity.

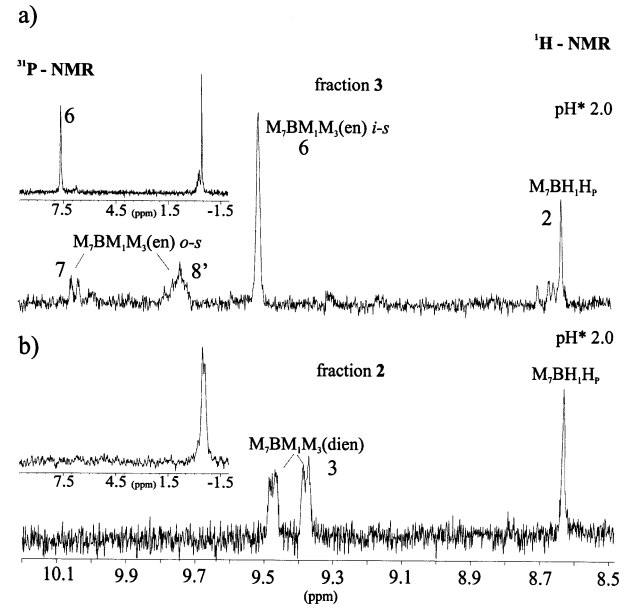

Fig. 18. ^1H and ^{31}P NMR spectra of the species $M_7BM_1M_3$(en) (fraction **3**) and $M_7BM_1M_3$(dien) (fraction **2**) following semi-preparative HPLC separation. The additional $M_7BH_1H_P$ resonance is in both cases due to a small degree of contamination through the central fraction **4**.

3. Conclusions

Our investigations confirm that intramolecular N–H···O(phosphate) hydrogen bonding plays a decisive role in enhancing specific interactions of (amine)M(II) (M = Pd, Pt) complexes with both purine nucleoside 2′- and 5′-monophosphates. In contrast, no potentiometric or NMR spectroscopic evidence for a similar outer-sphere phosphate participation in Group 10 metal binding to endocyclic purine N-atoms was obtained for $3'\text{-}AMP^{2-}$ or $3'\text{-}GMP^{3-}$.

As established by Martin et al. [1,11], the additional stabilisation of the N7 coordination mode for mononuclear (dien)Pd(II) complexes of $5'\text{-}AMP^{2-}$ or $5'\text{-}GMP^{3-}$ due to κ^2N7, *O*(phosphate) outer-sphere macrochelation is just sufficient to outweigh the stronger basicity of N1. The absence of such a specific interaction for the analogous nucleoside 2′- and 3′-monophosphates leads to a reversal in the intrinsic binding ratio log $[\beta(MB_1)/\beta(M_7B)]$ from −0.1 for $5'\text{-}AMP^{2-}$ to respectively 0.4 and 0.6 for $2'\text{-}AMP^{2-}$ and $3'\text{-}AMP^{2-}$. A similar change is also observed for guanosine monophosphates for which the respective intrinsic binding ratios are −0.2, 0.3 and 0.4. κ^2N7,O(phosphate) outer-sphere macrochelation is also responsible for the formation of a characteristic μ-*N1*,*N7* bridged cyclic tetramer $[\{(en)Pd(5'\text{-}GMP)\}_4]^{4-}$ with alternating $\kappa^2N7,N7'$ and $\kappa^2N1,N1'$ coordination of the participating (en)Pd(II) fragments. This predominance of a specific oligomer is in striking contrast to $2'\text{-}GMP^{3-}$ or $3'\text{-}GMP^{3-}$ for which a large number of μ-*N1*,*N7* bridged oligomers of differing nuclearities are observed for the (en)Pd(II) fragment in the same pH* range (5.5–9.5).

When an excess of the metal fragment is present, both inner- and outer-sphere κ^2N3,O(phosphate) macrochelation lead to a dramatic enhancement of (amine)M(II) binding to N3 of $2'\text{-}GMP^{3-}$ in comparison to 3′- and 5′-GMP^{3-}. Reaction of $[\{Pt(dien)\}_2(2'\text{-}GMP\text{-}\mu\text{-}N1,N7)]^+$ with $[Pt(en)(H_2O)_2]^{2+}$ affords both types of macroche-

late namely, $M_7BM_1M_{3,P}(en)$*i-s* and $M_7BM_1M_3(en)$*o-s*, with respectively direct (en)Pt–O(phosphate) binding and outer-sphere N–H···O(phosphate) hydrogen bonding. Neither type of κ^2N3,O(phosphate) macrochelate is formed by 3′-GMP^{3-} or 5′-GMP^{3-} under similar reaction conditions. Our spectroscopic characterisation of the inner-sphere species $M_7BM_1M_{3,P}(en)$*i-s* (**6**) for 2′-GMP^{3-} confirms Sigel's previous conclusion [12,13] that purine nucleoside 2′-monophosphates in their preferred *anti* conformation at the N9-C1′ glycosidic bond should be 'perfectly suited for this type of macrochelate formation'.

4. Experimental

Proton and ^{31}P NMR spectra were recorded in D_2O solutions on a Bruker DRX-400 spectrometer with sodium 3-(trimethylsilyl)tetradeuteriopropionate and 85% H_3PO_4 (external) as respective chemical shift references. FAB mass spectra were measured on a Fisons VG Autospec, with 3-nitrobenzylalcohol as the matrix, and ESI mass spectra on a Finnigan MAT 95 instrument. The starting materials [PdCl(dien)]Cl, [PtCl(dien)]Cl, [$PdCl_2$(en)] and [$PtCl_2$(en)] were prepared according to literature procedures [24–27]. Stock solutions of the aqua complexes $[M(dien)(H_2O)](NO_3)_2$ and $[M(en)(H_2O)_2](NO_3)_2$ (M = Pd, Pt) at suitable concentrations for ^1H NMR titrations (5–30 mmol l^{-1}), potentiometric titrations (0.5–3 mmol l^{-1}) and HPLC separations (analytical: 1 mmol l^{-1}, semipreparative: 10 mmol l^{-1}), were obtained by addition of 1.99 equivalents of $AgNO_3$ to an H_2O/D_2O solution of the appropriate chloride. After stirring for 24 h in the dark, the AgCl precipitate was removed by centrifugation and the volume of the resulting solution adjusted as required. The adenine and guanine nucleotides were purchased from Sigma Chemie GmbH and used as received.

4.1. Stability constant measurements

Potentiometric titrations were performed under argon with carbonate-free NaOH (0.1 mmol l^{-1}) in a thermostatted vessel (25 ± 0.1 °C) using 1.0 mmol l^{-1} nucleotide solutions at M:B ratios of 0.5, 1.0 and 3.0 as required for M = $[Pd(dien)(H_2O)](NO_3)_2$, $[Pd(en)(H_2O)_2](NO_3)_2$. This nucleotide concentration guarantees [19] that base stacking is negligible and therefore that the properties of the monomeric species are indeed studied. A fully automated microprocessor-controlled pH-titration unit (Metrohm 691 with Dosimat 665) was employed. A double-junction glass electrode (Metrohm 6.0219.100) containing a saturated KNO_3 solution between the membrane of the internal silver chloride reference electrode and an outer membrane was used to prevent diffusion of chloride ions into the titration solution. The pH meter was calibrated with standard buffer solutions (Riedel-de Haën: pH 4.008, 9.180). The use of such buffer solutions means that the measured pH value (pH_{meas}) will depend on the glass electrode, the junction potential, the background ionic strength I (0.1 mol l^{-1}, KNO_3) and the activity constant of H^+ [28,29]. As proposed by Sigel et al. [29], the conversion factor $A(=pH_{meas}-p[H]_{calc/conc})$ for adjustments between the practical (pH_{meas}) and concentration ($p[H]_{calc/conc}$) scales was determined by pointwise evaluation of titration curves of 0.1 mol l^{-1} HNO_3 (0.8 ml) and 0.1 mol l^{-1} KNO_3 (25 ml) with 0.1 mol l^{-1} NaOH. A value of A = 0.047(6), which falls within the range of previously reported values [28,29] was obtained on averaging all such 42 calibrations performed in this work. Use of Gran plots provided an average pK_w value of 13.93(3) for these measurements. Protonation and stability constants were calculated with HYPERQUAD [21] and MINIQUAD (for $[Pd(en)(H_2O)_2]^{2+}$/5′-GMP^{3-}) [30]. ^1H NMR titrations were performed with the same equipment as employed for potentiometric studies using procedures described previously [31]. Theoretical distribution curves for microspecies were calculated with log β values obtained from a least-squares refinement (program NIBIP96 [20]) against experimental resonance integral values.

4.2. HPLC

The analytical separations were performed with the following chromatographic equipment: Merck L-6200A pump, Rheodyne 7125 sample injector, Merck L-4250 variable-wavelength detector. Semipreparative work was carried out with a Knauer 64 pump and Merck L-4000A UV detector. Integration and evaluation were performed with the KNAUER EUROCHROM 2000 software package. Reversed-phase columns (25 × 0.4 cm inside diameter) for analytical separations were packed with Nucleosil 100-C_{18} (5μm, Macherey–Nagel); 25 × 2 cm inside diameter reversed phase columns (Nucleosil 100-C_{18}, 10μm) were employed for semipreparative work. Respective nucleotide concentrations of 1 mmol l^{-1} and 10mmol l^{-1} were present in the $[Pt(dien)(H_2O)]^{2+}$/$[Pt(en)H_2O)_2]^{2+}$/X′-GMP^{3-} reaction mixtures at 2.5/1/1 composition. Samples were run isocratically using 83% water–17% methanol as the mobile phase in the presence of 0.1% (v/v) pentafluoropropanoicacid (PFP) as an ion pairing agent. This led to pH value of 2.1 ± 0.1 for the mobile phase. Analytical HPLC was run at a flow rate of 1 ml min^{-1}, semipreparative HPLC at 36 ml min^{-1}. Peak detection was performed by UV absorption at 220 nm.

Acknowledgements

The authors are grateful to the Deutsche Forschungsgemeinschaft and the Fonds der Chemischen Industrie for financial support.

References

[1] K.H. Scheller, V. Scheller-Krattiger, R.B. Martin, J. Am. Chem. Soc. 103 (1981) 6833.
[2] M.D. Reily, T.W. Hambley, L.G. Marzilli, J. Am. Chem. Soc. 110 (1988) 2999.
[3] K. Uchida, A. Toyama, Y. Tamura, M. Sugimura, F. Mitsomori, Y. Furukawa, H. Takeuchi, I. Harada, Inorg. Chem. 28 (1989) 2067.
[4] S.J. Berners-Price, U. Frey, J.D. Ranford, P.J. Sadler, J. Am. Chem. Soc. 115 (1993) 8649.
[5] K.J. Barnham, C.J. Bauer, M.I. Djuran, M.A. Mazid, T. Rau, P.J. Sadler, Inorg. Chem. 34 (1995) 2826.
[6] T. Rau, R. van Eldik, Chem. Ber. 130 (1997) 1551.
[7] Z. Guo, P.J. Sadler, E. Zang, Chem. Commun. (1997) 27.
[8] M. Green, M. Garner, D.M. Orten, Trans. Met. Chem. 17 (1992) 164.
[9] A.T.M. Marcelis, O. Erkelens, J. Reedijk, Inorg. Chim. Acta 91 (1984) 129.
[10] D.J. Evans, M. Green, R. van Eldik, Inorg. Chim. Acta 128 (1987) 27.
[11] U.K. Häring, R.B. Martin, Inorg. Chim. Acta 80 (1983) 1.
[12] S.S. Massoud, H. Sigel, Eur. J. Biochem. 179 (1989) 451.
[13] H. Sigel, Chem. Soc. Rev. 22 (1993) 255.
[14] C.A. Blindauer, A.H. Emwas, A. Holý, H. Dvořáková, E. Sletten, H. Sigel, Chem. Eur. J. 3 (1997) 1526.
[15] E. Yuriev, J.D. Orbell, Inorg. Chem. 37 (1998) 6269.
[16] G. Raudaschl-Sieber, H. Schöllhorn, U. Thewalt, B. Lippert, J. Am. Chem. Soc. 107 (1985) 3591.
[17] W.S. Sheldrick, B. Günther, Inorg. Chim. Acta 152 (1988) 223.
[18] C. Meiser, B. Song, E. Freisinger, M. Peilert, H. Sigel, B. Lippert, Chem. Eur. J. 3 (1997) 388.
[19] H. Sigel, S.S. Massoud, N.A. Corfu, J. Am. Chem. Soc. 116 (1994) 2958.
[20] J. Blotevogel-Baltronat, Dissertation, Ruhr-Universität Bochum, Bochum, 1997.
[21] A. Sabatini, A. Vacca, P. Gans, Talanta 43 (1996) 1739.
[22] M.D. Reily, L.G. Marzilli, J. Am. Chem. Soc. 108 (1986) 6785.
[23] S. Yao, J.P. Plastaras, L.G. Marzilli, Inorg. Chem. 33 (1994) 6061.
[24] F. Basolo, H.B. Gray, R.B. Pearson, J. Am. Chem. Soc. 82 (1960) 4200.
[25] G. Annibale, M. Brandolisio, B. Pitteri, Polyhedron 14 (1995) 451.
[26] B.J. McCormik, E.N. Jaynes, R.I. Kaplan, Inorg. Synth. 13 (1972) 216.
[27] L.F. Heneghan, J.C. Bailar, Jr., J. Am. Chem. Soc. 75 (1953) 1840.
[28] H.M. Irving, M.G. Miles, L.D. Pettit, Anal. Chim. Acta 38 (1967) 475.
[29] H. Sigel, A.D. Zuberbühler, O. Yamauchi, Anal. Chim. Acta 255 (1991) 63.
[30] A. Sabatini, A. Vacca, P. Gans, Talanta 21 (1974) 53.
[31] D. Neumann, W.S. Sheldrick, Inorg. Chim. Acta 223 (1994) 131.